# Direct production of a light *CP*-odd Higgs boson at the Tevatron and LHC

Radovan Dermíšek

*Department of Physics, Indiana University, Bloomington, Indiana 47405, USA*

John F. Gunion

*Department of Physics, University of California, Davis, California 95616, USA*
*and Theory Group, CERN, CH-1211, Geneva 23, Switzerland*

We show that the existing CDF $L = 630$ pb$^{-1}$ Tevatron data on $pp \rightarrow \mu^+ \mu^- X$ places substantial limits on a light *CP*-odd Higgs boson $a$ with $m_a < 2m_B$ produced via $gg \rightarrow a$, even for $m_a > 2m_\tau$ for which BR($a \rightarrow \mu^+ \mu^-$) is relatively small. Extrapolation of this existing CDF analysis to $L = 10$ fb$^{-1}$ suggests that Tevatron limits on the $ab\bar{b}$ coupling strength in the region $m_a > 8$ GeV could be comparable to or better than limits from Upsilon decays in the $m_a < 7$ GeV region. We also give rough estimates of future prospects at the LHC, demonstrating that early running will substantially improve limits on a light $a$ (or perhaps discover a signal). In particular, outside the Upsilon peak region, integrated luminosity of only 5 fb$^{-1}$–20 fb$^{-1}$ (depending on $m_a$ and $\sqrt{s}$) could reveal a peak in $M_{\mu^+ \mu^-}$ and will certainly place important new limits on a light $a$. The importance of such limits in the context of next-to-minimal supersymmetric model Higgs discovery and $(g - 2)_\mu$ are outlined.

## I. INTRODUCTION

Many motivations for the existence of a light *CP*-odd Higgs boson, $a$, have emerged in a variety of contexts in recent years. Of particular interest is the $m_a < 2m_B$ region, for which a light Higgs, $h$, with SM-like $WW$, $ZZ$ and fermionic couplings can have mass below the nominal LEP limit of $m_h > 114$ GeV by virtue of $h \rightarrow aa \rightarrow 4\tau$ decays being dominant [1–4] (see also [5,6]). For $m_h \lesssim 105$ GeV, the Higgs provides perfect agreement with the rather compelling precision electroweak constraints, and for BR($h \rightarrow aa$) $\gtrsim 0.75$ also provides an explanation for the $\sim 2.3\sigma$ excess observed at LEP in $e^+ e^- \rightarrow Zb\bar{b}$ in the region $M_{b\bar{b}} \sim 100$ GeV if $m_h \sim 100$ GeV. This is sometimes referred to as the "ideal" Higgs scenario. More generally, superstring modeling suggests the possibility of many light $a$'s, at least some of which couple to $\mu^+ \mu^-$, $\tau^+ \tau^-$, and $b\bar{b}$. Further, it is not excluded that a light $a$ with $m_a > 8$ GeV and enhanced $ab\bar{b}$ coupling could be responsible for the deviation of the measured muon anomalous magnetic moment $a_\mu$ from the SM prediction [7]. Below, we will show that a light $a$ with the required $ab\bar{b}$ and $a\mu^+ \mu^-$ couplings would have been seen in existing Tevatron data for the $\mu^+ \mu^-$ final state at low $M_{\mu^+ \mu^-}$. More generally, current muon pair Tevatron data places significant limits on a light $a$. These will be further strengthened with increased Tevatron integrated luminosity and by $\mu^+ \mu^-$ data obtained at the LHC.

The possibilities for discovery of an $a$ and limits on the $a$ are phrased in terms of the $a\mu^- \mu^+$, $a\tau^- \tau^+$, $ab\bar{b}$, and $at\bar{t}$ couplings defined via

$$\mathcal{L}_{af\bar{f}} \equiv iC_{af\bar{f}} \frac{ig_2 m_f}{2m_W} \bar{f}\gamma_5 fa. \tag{1.1}$$

In this paper, we assume a Higgs model in which $C_{a\mu^- \mu^+} = C_{a\tau^- \tau^+} = C_{ab\bar{b}}$, as typified by a two-Higgs-doublet model (2HDM) of either type-I or type-II, or more generally if the lepton and down-type quark masses are generated by the same combination of Higgs fields. However, one should keep in mind that there are models in which $r = (C_{a\mu^- \mu^+} = C_{a\tau^- \tau^+})/C_{ab\bar{b}} \gg 1$—such models include those in which the muon and tau masses are generated by different Higgs fields than the $b$ mass. In a 2HDM of type-II and in the MSSM, $C_{a\mu^- \mu^+} = C_{a\tau^- \tau^+} = C_{ab\bar{b}} = \tan\beta$ (where $\tan\beta = h_u/h_d$ is the ratio of the vacuum expectation values for the doublets giving mass to up-type quarks vs down-type quarks) and $C_{at\bar{t}} = \cot\beta$. These results are modified in the next-to-minimal supersymmetric model (NMSSM) (see, e.g. [8,9]).[1] In the NMSSM, both $C_{at\bar{t}}$ and $C_{ab\bar{b}} = C_{a\mu^- \mu^+} = C_{a\tau^- \tau^+}$ are multiplied by a factor $\cos\theta_A$, where $\cos\theta_A$ is defined by

$$a = \cos\theta_A a_{MSSM} + \sin\theta_A a_S, \tag{1.2}$$

where $a$ is the lightest of the 2 *CP*-odd scalars in the model (sometimes labeled as $a_1$). Above, $a_{MSSM}$ is the *CP*-odd (doublet) scalar in the MSSM sector of the NMSSM and $a_S$ is the additional *CP*-odd singlet scalar of the NMSSM. In terms of $\cos\theta_A$, $C_{a\mu^- \mu^+} = C_{a\tau^- \tau^+} = C_{ab\bar{b}} = \cos\theta_A \tan\beta$

---

[1]A convenient program for exploring the NMSSM Higgs sector is NMHDECAY [10,11].

and $C_{a t \bar{t}} = \cos\theta_A \cot\beta$. Quite small values of $\cos\theta_A$ are natural when $m_a$ is small as a result of being close to the $U(1)_R$ limit of the model. In the most general Higgs model, $C_{a \mu^- \mu^+}$, $C_{a \tau^- \tau^+}$, $C_{a b \bar{b}}$, and $C_{a t \bar{t}}$ will be more complicated functions of the vevs of the Higgs fields and the structure of the Yukawa couplings. In this paper, we assume $C_{a \mu^- \mu^+} = C_{a \tau^- \tau^+} = C_{a b \bar{b}}$ and $C_{a b \bar{b}}/C_{a t \bar{t}} = \tan^2\beta$.

One should keep in mind, however, the fact that the above are tree-level couplings and that the $b\bar{b}a_{\mathrm{MSSM}}$ coupling is especially sensitive to radiative corrections from SUSY particle loops that can be large when $\tan\beta$ is large [12–14]. These are typically characterized by the quantity $\Delta_b$ which is crudely of order $\frac{\mu \tan\beta}{16\pi^2 M_{\mathrm{SUSY}}}$. The correction to the coupling then takes the form of $1/(1 + \Delta_b)$. Since $\mu$ can have either sign, $C_{a b \bar{b}}$ can be either enhanced or suppressed relative to equality with $C_{a \tau^- \tau^+}$ (the corrections to which are much smaller) and $C_{a \mu^- \mu^+}$ (the corrections to which are negligible).

In the past, probes of a light $a$ have mainly relied on production of a primary particle (e.g. an Upsilon) which then decays to a lighter $a$ with the emission of a known SM particle (e.g. a photon). Such probes are strictly limited to a maximum accessible $m_a$ by simple kinematics. The only exceptions to this statement have been probes based on $e^+e^- \to b\bar{b}a$ followed by $a \to \tau^+\tau^-$ or $a \to b\bar{b}$, with LEP providing the strongest (but still rather weak) limits on the $a$ based on this type of radiative production process.

In contrast, hadron colliders potentially have a large reach in $m_a$ as a result of the fact that an $a$ can be produced via $gg \to a$. The $gga$ coupling derives from quark triangle loops. This process, plus higher order corrections thereto, leads to a large cross section for the $a$ due to the large $gg$ "luminosity" at small gluon momentum fractions, provided the $aq\bar{q}$ coupling deriving from the doublet component of the $a$ is significant. This large cross section will typically lead to a significant number of $gg \to a \to \mu^+\mu^-$ events even though $\mathrm{BR}(a \to \mu^+\mu^-)$ is not very large (and in fact is quite small for $m_a > 2m_\tau$). Further, since the $a$ is a very narrow resonance, all $a$ events will typically fall into a single bin of size given by the $M_{\mu^+\mu^-}$ mass resolution of the experiment, typically below 100 MeV. This implies very controllable background levels, mostly deriving from heavy flavor production (e.g. $b\bar{b}$ and $c\bar{c}$), once isolation and promptness cuts have been imposed on the muons.

The Higgs doublet component of the $a$ can be suppressed when the $a$ mixes with one or more SM singlet $CP$-odd field, e.g. the $a_S$ of the NMSSM as made explicit above. However, what is important for limits is $C_{a b \bar{b}}$. In the NMSSM context, the scenarios allowing a light scalar Higgs to escape LEP limits by virtue of $h \to aa$ decays with $m_a < 2m_B$ are such that $\cos\theta_A$ is only small when $\tan\beta$ is large; for example, preferred scenarios for $\tan\beta = 10$ are such that $\cos\theta_A \sim 0.1$, implying $C_{a b \bar{b}} \sim 1$. As a result, the Tevatron and LHC provide very significant probes of such a light $a$ despite its being only 1% doublet

(at the probability level). In addition, there are models beyond the MSSM [15,16], including scenarios within the NMSSM [17], in which the doublet component of the $a$ can be quite substantial. (For a review, see also [18].) In such models there are typically several Higgs scalars (including charged Higgs bosons) with masses near 100 GeV that have escaped discovery because of decays involving the light $a$. This type of scenario requires that $\tan\beta$ be small ($1 \lesssim \tan\beta \lesssim 3$). When the doublet component of the $a$ is substantial $C_{a b \bar{b}} = \cos\theta_A \tan\beta$ will have magnitude $\gtrsim 1$ and hadron colliders will almost certainly discover or exclude the $a$. In the case of the NMSSM, there is a portion of the preferred parameter region for low $\tan\beta$ in which precisely this kind of scenario arises. However, in the NMSSM at low $\tan\beta$ there is a second part of the preferred parameter region in which there are many light Higgs bosons but the $a$ is mainly singlet. In this latter case, $|C_{a b \bar{b}}|$ will be relatively small and direct searches for the light $a$ will be more difficult than in NMSSM models with larger $\tan\beta$.

The organization of the paper is as follows. In Sec. II, we review some basic facts about a light $a$ and limits on $C_{a b \bar{b}} = C_{a \mu^- \mu^+} = C_{a \tau^- \tau^+}$ coming from non–hadron-collider data. In Sec. III, we discuss the additional limits that can be placed on the couplings of the $a$ implied by existing Tevatron analyses and data and extrapolate these existing results to $L = 10$ fb$^{-1}$ data sets. In Sec. IV, we analyze prospects for discovering, or at least further improving limits on the couplings of, a light $a$ using early LHC data. Section V summarizes our conclusions and provides a few additional comments.

## II. PHENOMENOLOGY AND LIMITS FOR A LIGHT $CP$-ODD $a$

One key ingredient in understanding current limits and future prospects is the branching ratio for $a \to \mu^+\mu^-$ decays. This branching ratio (which is independent of $\cos\theta_A$ at tree-level due to the absence of tree-level $a \to VV$ couplings and similar) is plotted in Fig. 1. Note that $\mathrm{BR}(a \to \mu^+\mu^-)$ changes very little with increasing $\tan\beta$ at any given $m_a$ once $\tan\beta \gtrsim 2$.

Limits on $|C_{a b \bar{b}}| = |\cos\theta_A| \tan\beta$ were analyzed in [7] (see also [19]), based on data available at the time. The analysis of [7] employed limits from $\Upsilon \to \gamma a$ decays, the importance of which was emphasized in [20] (especially within the NMSSM context), as well as from $e^+e^- \to b\bar{b}a$ production at LEP. The analysis of [7] was done prior to the very recently released *BABAR* $\Upsilon(nS) \to \gamma a$ results [21,22]. Without including the $\Upsilon_{3S}$ *BABAR* data, limits in the 8 GeV $< m_a < 2m_B$ range (especially, $M_{\Upsilon_{1S}} < m_a < 2m_B$) are quite weak and suffer from uncertainty regarding $\eta_b - a$ mixing. An update employing the $\Upsilon_{3S}$ data will be performed in a separate paper. In the present paper, the limits implicit in Tevatron data are compared to the limits obtained in [7]. We will also briefly summarize how this
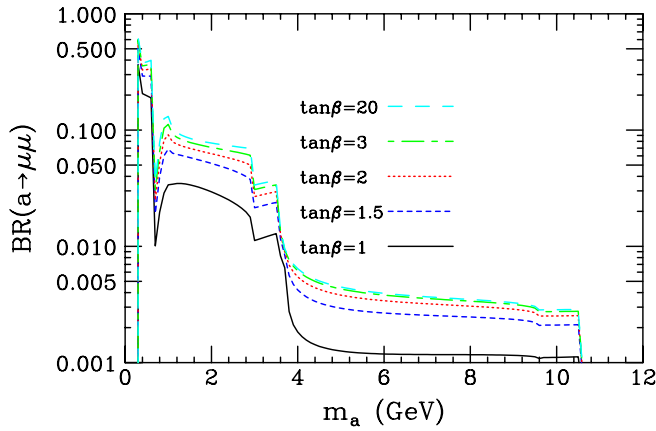
FIG. 1 (color online). BR($a \to \mu^+ \mu^-$) is plotted as a function of $m_a$ for a variety of $\tan\beta$ values. BR($a \to \mu^+ \mu^-$) is independent of $\cos\theta_A$ at tree-level.

comparison will change after inclusion of the $\Upsilon_{3S}$ *BABAR* results.

Focusing on the NMSSM, we note that it is always possible to choose $\cos\theta_A$ so that the limits on $C_{ab\bar{b}}$ as a function of $\tan\beta$ are satisfied. The maximum allowed value of $|\cos\theta_A|$, $\cos\theta_A^{max}$, as a function of $m_a$ for various $\tan\beta$ values as obtained in [7] is plotted in Fig. 2. Constraints are strongest for $m_a \lesssim 7$ GeV for which Upsilon limits are strong, and deteriorate rapidly above that.

Turning to the 2HDM(II), where $C_{ab\bar{b}} = \tan\beta$, we note that any point for which $\cos\theta_A^{max}$ is smaller than 1 corresponds to an $m_a$ and $\tan\beta$ choice that is not consistent with the experimental limits. Disallowed regions emerge for
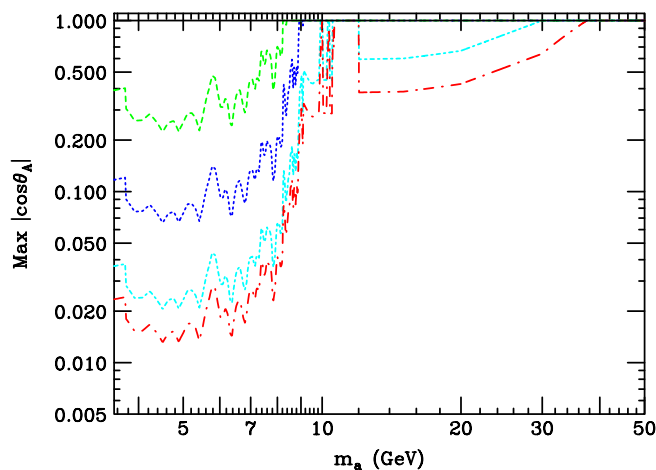


FIG. 2 (color online). We plot results from [7] for $\cos\theta_A^{max}$ in the NMSSM (where $C_{ab\bar{b}} = \cos\theta_A \tan\beta$) as a function of $m_a$ for $m_a > 2m_\tau$. The different curves correspond to $\tan\beta = 1$ (upper curve), 3, 10, 32 and 50 (lowest curve). The region between $\sim 2m_\tau$ and $\sim 8$ GeV is strongly constrained by CLEO III data [35] on $\Upsilon_{1S} \to \gamma\tau^+\tau^-$ decays. The plotted limits do not include the *BABAR* $\Upsilon_{3S} \to \gamma\tau^+\tau^-$ and $\Upsilon_{3S} \to \gamma\mu^+\mu^-$ limits that became available after the analysis of [7].

$m_a \lesssim 10$ GeV at higher $\tan\beta$. A disallowed region also arises over a limited $m_a$ range starting from $m_a > 12$ GeV when $\tan\beta \gtrsim 18$, the larger the value of $\tan\beta$ the larger the interval. For example, for $\tan\beta = 50$ the 2HDM(II) is not consistent for $m_a < 10$ GeV nor for $12 \lesssim m_a \lesssim 37$ GeV. In contrast, for $\tan\beta = 10$ the 2HDM(II) model is only inconsistent for $m_a \lesssim 9$ GeV.

Before proceeding, we note that constraints from precision electroweak data are easily satisfied for a light $a$ in both the 2HDM(II) and NMSSM cases (see [7] for more discussion). We also wish to make note of the regions of interest for obtaining a new physics contribution, $\Delta a_\mu$, of order $\Delta a_\mu \sim 27.5 \times 10^{-10}$ (the current discrepancy between observation and the SM prediction). These can be roughly described as follows. In the 2HDM(II) context, such $\delta a_\mu$ requires a rather precisely fixed value of $\tan\beta \sim$ 30–32 and $m_a \sim 9.9$–12 GeV. In the NMSSM context, the strong constraints from Upsilon physics imply that significant contributions to $a_\mu$ are not possible until $m_a$ exceeds roughly 9.2 GeV. The maximal $\delta a_\mu$ can exceed $\Delta a_\mu \equiv 27.5 \times 10^{-10}$ for 9.9 GeV $\lesssim m_a \lesssim 12$ GeV if $\tan\beta \geq 32$, with an almost precise match to this value for $\tan\beta = 32$. For $\tan\beta = 50$, one can match $\Delta a_\mu$ by using a value of $\cos\theta_A$ below $\cos\theta_A^{max}$. (The fact that matching is possible for 9.9 GeV $\lesssim m_a \lesssim 2m_B$ is particularly interesting in the context of the ideal Higgs scenario.) Further, the maximal $\delta a_\mu$ is in the $7$–$20 \times 10^{-10}$ range for 12 GeV $< m_a \lesssim$ 48 GeV for $\tan\beta = 32$ and for 12 GeV $< m_a \lesssim 70$ GeV for $\tan\beta = 50$.

At this point, it is worth discussing in more depth the ideal $m_h \sim 100$ GeV, $m_a \lesssim 2m_B$, BR($h \to aa$) $> 0.75$ Higgs scenario as discussed in [1–4]. These references examined the degree to which obtaining the observed value of $m_Z$ requires very precisely tuned values of the grand unified theory (GUT) scale parameters of the MSSM and NMSSM. One finds that in any supersymmetric model this fine-tuning is always minimized for GUT scale parameters that yield a SM-like $h$ with $m_h \lesssim 100$–105 GeV, something that is only consistent with LEP data if the $h$ has unexpected decays that reduce the $h \to b\bar{b}$ branching ratio while not contributing to $h \to b\bar{b}b\bar{b}$ (also strongly constrained by LEP data). A Higgs sector with a light $a$ for which BR($h \to aa$) $> 0.75$ and with $m_a$ small enough that $a$ decays to $B\bar{B}$ final states are disallowed (i.e. $m_a <$ 10.56 GeV) provides a very natural possibility for allowing minimal fine-tuning. The NMSSM provides one possible example. As a useful benchmark, in the context of the NMSSM the $\tan\beta = 10$ scenarios that yield the required $m_a < 2m_B$ and BR($h \to aa$) $> 0.75$ are ones with $0.35 \gtrsim$ $|C_{ab\bar{b}}|$ ($|\cos\theta_A| \gtrsim 0.035$). The lower limit arises from the fact that BR($h \to aa$) falls below the 0.75 level needed for the ideal Higgs scenario if $|\cos\theta_A|$ is too small. From Fig. 2 we see that such $|\cos\theta_A|$ values are not yet excluded for any $m_a > 2m_\tau$. This range becomes more restricted if, in addition, one requires small fine-tuning of the $A_\lambda$ and $A_\kappa$

TABLE I. Values of $\cos\theta_A$ required for $m_a < 2m_B$ and sufficiently large BR($h \to aa$) to escape LEP limits on the $Zb\bar{b}$ final state. Results both without and with $G < 20$ required are presented for a selection of $\tan\beta$ values.

| $\tan\beta$ | $\cos\theta_A$ ranges | $\cos\theta_A$ ranges, $G < 20$ required |
|---|---|---|
| 1.7 | $< -0.3$ or $>0.1$ | $[-0.6, -0.5]$ or $\sim +0.1$ |
| 2 | $< -0.3$ or $>0.1$ | $[-0.7, -0.5]$ |
| 3 | $< -0.06$ | $[-0.35, -0.08]$ |
| 10 | $< -0.06$ or $>0.035$ | $[-0.12, -0.08]$ or $[0.06, 0.08]$ |
| 50 | $< -0.04$ or $>0.04$ | $[-0.06, -0.04]$ or $\sim +0.04$ |

soft-SUSY-breaking NMSSM parameters that determine the properties of the $a$—such fine-tuning is characterized by a parameter we call $G$, defined in [3]. At $\tan\beta = 10$, $0.6 \lesssim |C_{ab\bar{b}}| \lesssim 1.2$ ($0.06 \lesssim |\cos\theta_A| \lesssim 0.12$) is required if $G < 20$ is imposed as well as requiring $m_a < 2m_B$ and BR($h \to aa$) > 0.75. For $\tan\beta \lesssim 2$, the means for escaping the LEP constraints on the light scalar Higgses are a bit more complex since two $\sim 100$ GeV Higgses can share the ZZ-Higgs couplings squared, but there is always a lower limit on $|\cos\theta_A|$ for which such escape is possible. In Table I, we tabulate more precisely the values of $\cos\theta_A$ for various $\tan\beta$ values that: a) have $m_a < 2m_B$ and large enough BR($h \to aa$) to escape LEP limits on the $h$, with no constraint on $G$; and b) have small $A_\kappa$, $A_\lambda$ fine-tuning measure $G < 20$ as well as $m_a < 2m_B$ and large enough BR($h \to aa$).

We can summarize the implications of this table as follows. First, comparing to the existing limits on $|\cos\theta_A|$ as plotted in Fig. 2, we see that only ideal Higgs scenarios (i.e. ones with $m_h < 105$ GeV and BR($h \to aa$) large enough to escape LEP limits) with $\tan\beta > 30$ and $m_a \lesssim 8$ GeV are excluded. Ideal Higgs scenarios with $\tan\beta < 10$ are fairly far from being excluded. If we wish to eliminate ideal Higgs scenarios then: for $1.7 \lesssim \tan\beta \lesssim 2$,[2] we must exclude $|C_{ab\bar{b}}| \gtrsim 0.17$; for $\tan\beta = 3$, we must exclude $|C_{ab\bar{b}}| \gtrsim 0.18$; for $\tan\beta = 10$, we must exclude $|C_{ab\bar{b}}| \gtrsim 0.35$ and for $\tan\beta = 50$, we must exclude $|C_{ab\bar{b}}| \gtrsim 2$. If we only wish to exclude such scenarios that also have $G < 20$, then the required $|C_{ab\bar{b}}|$ levels for $\tan\beta = 1.7, 2, 3, 10, 50$ are 0.17, 1, 0.24, 0.6, 2, respectively. As we shall see, completely probing even the latter levels for all $m_a < 2m_B$ will be challenging, but hadron colliders may ultimately play a leading role. Indeed, those scenarios with $G < 20$ typically have $m_a$ values above 7.5 GeV and most often above $M_{\Upsilon_{3S}}$. Of course, the many scenarios with larger $|\cos\theta_A|$ than the values listed above will be correspondingly easier to exclude or verify.

Finally, we comment on the implications of the recent preliminary ALEPH results [23] which place a limit on

$$\xi^2 \equiv \frac{\sigma(e^+e^- \to Zh)}{\sigma(e^+e^- \to Zh_{SM})} \text{BR}(h \to aa)[\text{BR}(a \to \tau^+\tau^-)]^2$$

(2.1)

as a function of $m_h$ and $m_a$. Very roughly, $\xi^2 \lesssim 0.4$ at 95% CL for $m_a = 10$ GeV and $m_h = 100$ GeV. This limit is sufficient to (marginally) exclude the $m_h \sim 100$ GeV scenarios with $\tan\beta \geq 3$, since these predict $\xi^2 \sim$ 0.42–0.43 at larger $m_a \lesssim 2m_B$. However, for $\tan\beta \lesssim 2$, predicted $\xi^2$ values for the ideal NMSSM Higgs scenarios are $\lesssim 0.3$ and such scenarios are fully consistent with the new ALEPH limits. The value of $\xi^2$ declines at lower $\tan\beta$ values because more of the $a$ decays are to final states such as $gg$, $c\bar{c}$ and $s\bar{s}$. For the consequent $h$ decay final states, LEP limits on $m_h$ are no better than 82 GeV. If one allows for $m_h$ as large as 105 GeV, then the ALEPH limits are much weaker, excluding only $\xi^2 < 0.62$ for $m_a = 10$ GeV. Scenarios with $\tan\beta = 10$, $m_h \sim 105$ GeV, minimal electroweak and light-$a$ fine-tuning and $\xi^2 \sim 0.43$ are not uncommon for $m_a \lesssim 2m_B$. (In contrast, at $\tan\beta = 3$ electroweak fine-tuning is only small if $m_h < 100$ GeV.) Details will be provided in a forthcoming paper [24].

## III. THE ROLE OF THE TEVATRON

Potentially, the Tevatron can probe precisely the $m_a$ range close to and above the $\Upsilon(nS)$ masses which cannot be probed in $\Upsilon(nS)$ decays. Some relevant analyzes have been performed looking for a very narrow resonance, denoted $\epsilon$, that is produced in the same way as the $\Upsilon_{1S}$. The published/preprinted results are those of [25,26] from the CDF experiment. The latter results employ data corresponding to $L = 630$ pb$^{-1}$ and exclude the potential $\epsilon$ peak at $M_{\mu^+\mu^-} \sim 7.2$ GeV present in the $L = 110$ pb$^{-1}$ data of the first paper. The analysis was only performed for the region from 6.3 GeV $\leq M_{\mu^+\mu^-} \leq 9$ GeV. The reason for not performing the analysis at lower $M_{\mu^+\mu^-}$ is that the acceptance of the $\mu^+\mu^-$ pair relative to that of the $\Upsilon_{1S}$ (used as a normalizing cross section) would be highly mass dependent. This is due to the fact that CDF is only able to see $\mu^+\mu^-$ pairs with $p_T > 5$ GeV and for $M_{\mu^+\mu^-} <$ 6.3 GeV the fraction of pairs that fail this cut becomes highly mass dependent. No reason for not analyzing the region of $M_{\mu^+\mu^-} > 9$ GeV is given, although it is in this region that the $\Upsilon(1S, 2S, 3S)$ peaks are present.

Our goal here is to use the above $\epsilon$ analyses to place limits on a $CP$-odd $a$. This is possible under certain assumptions detailed below. In particular, we will place limits on $C_{ab\bar{b}}$.

The dominant production mechanism for a light $a$ at a hadron collider is different than that for the $\epsilon$ (assumed to be the same or very similar in kinematic shape etc. for the $\Upsilon_{1S}$). The production mechanisms for the $\Upsilon_{1S}$ remain

---

[2]Scenarios with $\tan\beta$ much below 1.7 are problematical since it is difficult to retain perturbativity for Yukawa couplings all the way up to the unification scale.

uncertain. It has recently been claimed [27] that an NNLO version of the leading order (LO) calculation can reproduce the Tevatron results for direct production of the $\Upsilon_{1S}$ at larger $p_T$ (roughly $p_T > 5$ GeV). The diagrams employed begin with the LO $\mathcal{O}(\alpha_S^3)$ process $gg \to b\bar{b}g$ with the $b\bar{b}$ pair turning into the $\Upsilon_{1S}$ with probability determined by $|R_{\Upsilon_{1S}}(0)|^2$, leading to an $\Upsilon_{1S} + g$ final state. At NLO, the $\alpha_S^4$ diagrams include virtual correction diagrams that also lead to the $\Upsilon_{1S} + g$ final state and several diagrams containing an extra quark or gluon in the final state ($\Upsilon_{1S} + 2g$ and $\Upsilon_{1S} + b\bar{b}$). Several $\mathcal{O}(\alpha_S^5)$ diagrams leading to $\Upsilon_{1S} + 3j$ final states (especially $\Upsilon_{1S} + 3g$) are argued to be of importance at larger $p_T$ and are also included. Resummation [28] is necessary to get the low $p_T$ portion of the cross section. From CDF and D0 data, the direct $\Upsilon_{1S}$ production cross section is measured to be about 50% of the total. Indirect contributions coming from, for example, $gg \to \chi_b$ followed by $\chi_b \to \Upsilon_{1S}\gamma$ make up the remaining 50% of the total $\Upsilon_{1S}$ production rate. In contrast, $a$, being a spin-0 resonance, will be dominantly produced via $gg \to a$ through the quark-loop induced $gga$ coupling. In addition, there are large QCD corrections to the one-loop-induced cross section. These are of two basic types: (a) virtual corrections and soft gluon corrections; (b) corrections containing an extra resolvable gluon or quark in the final state (the dominant diagram is $gg \to ag$) in close proximity to the $a$. The total cross sections predicted by HIGLU [29] are plotted as a function of $m_a$ for $C_{ab\bar{b}} = 1/C_{at\bar{t}} = \tan\beta = 1$, 2, 3, 10 in Fig. 3 with and without the resolvable parton final state QCD corrections. The HIGLU results agree well with a private program for this process. We note that the cross sections do not scale precisely as $\tan^2\beta$ at large $\tan\beta$ (as naively predicted by dominance of the $b$-quark loop diagram for the $gg \to a$ coupling at high $\tan\beta$) due to the

virtual corrections. In any case, very substantial cross sections are predicted. In the NMSSM context, at any given $\tan\beta$ value one should reduce the plotted result for that $\tan\beta$ by a factor of $(\cos\theta_A)^2$.

Among the cuts employed in the CDF analysis there is an isolation requirement whereby events are only included if both muons have less than 4 GeV scalar summed $p_T$ in a cone of size $\Delta R = 0.4$ about the muon. The impact of the isolation requirement was studied for the $\Upsilon_{1S}$ and it was found that this isolation requirement was 99.8% efficient for the $\Upsilon_{1S}$ despite the fact that $\Upsilon_{1S}$'s are produced along with one or more extra particles in the final state. Thus, in our analysis for the $a$ we will make the assumption that the components of the $a$ cross section coming from final states containing an extra $q$ or $g$ are not significantly affected by the isolation cut and thus we will employ the full QCD-corrected $a$ cross section. In addition, in the analysis of [26] only events for which the $\mu^+\mu^-$ pair resides in the $|y| < 1$ region are retained. Thus, what we actually employ are the cross sections

$$\sigma(a)_{|y|<1} = \frac{d\sigma(a)}{dy}\bigg|_{y=0} \times 2, \qquad (3.1)$$

which is an excellent approximation given that the cross section is essentially flat in $y$ over this region. At the Tevatron, the ratio

$$\frac{\frac{d\sigma(a)}{dy}\big|_{y=0}}{\sigma(a)_{\text{tot}}} \qquad (3.2)$$

varies from roughly 0.12 at $m_a \sim 2$ GeV to 0.19 at $m_a \sim 12$ GeV with very weak dependence on $\tan\beta$. At $m_a = M_{\Upsilon_{1S}}$ the ratio is $\sim 0.15$.

In [26], what is given are limits on the ratio for production of a very narrow resonance, the $\epsilon$, relative to that for the $\Upsilon_{1S}$

$$R = \frac{\sigma(\epsilon)\text{BR}(\epsilon \to \mu^+\mu^-)}{\sigma(\Upsilon_{1S})\text{BR}(\Upsilon_{1S} \to \mu^+\mu^-)} \qquad (3.3)$$

under the assumption that the same mechanism is responsible for $\epsilon$ production as is responsible for $\Upsilon_{1S}$ production. As stated earlier, since the $a$ can be produced directly via $gg \to a$ whereas the $\Upsilon_{1S}$ cannot, an interpretation for the $a$ of the limits given for the generic $\epsilon$ requires actually knowing what the $\Upsilon_{1S}$ cross section is. It also requires an assumption regarding the efficiency for the $a$ of acceptance and isolation requirements relative to those employed for the $\epsilon$.

Our analysis is the following. In Ref. [25], it is stated that the cross section for $\Upsilon_{1S}$ production in the $|y| < 0.6$ region at $\sqrt{s} = 1.8$ TeV was measured to be 34 600 pb. In contrast, the cuts of Ref. [25] accept $\Upsilon_{1S}$ events with $|y| < 1$. In Ref. [25], it is stated that the efficiency for $\Upsilon_{1S}$ detection (due to geometric and kinematic acceptance cuts as well as trigger and reconstruction efficiencies, but
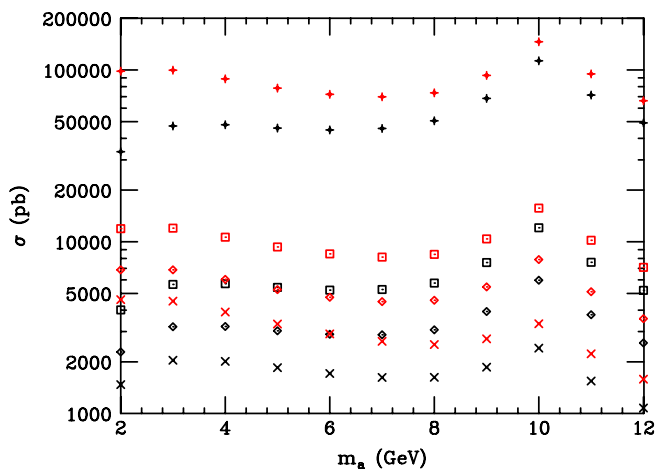


FIG. 3 (color online). The total cross section for $a$ production at the Tevatron is plotted vs $m_a$ for $\tan\beta = 1, 2, 3, 10$ (lowest to highest point sets). For each $m_a$ and $\tan\beta$ value, the lower (higher) point is the cross section without (with) resolvable parton final state contributions.

before imposing the isolation requirement noted above) is 0.066. From [30], we infer that this acceptance times efficiency factor is one that applies at any fixed value of $y$ that is relatively central and after integrating over accepted $p_T$'s. Then, using $\mathrm{BR}(\Upsilon_{1S} \to \mu^+ \mu^-) = 0.0248$ and the integrated luminosity of $L = 110 \text{ pb}^{-1}$ one then predicts

$$34600 \times \left(\frac{2}{1.2}\right) \times 110 \text{ pb}^{-1} \times 0.0248 \times 0.066 = 10\,383 \tag{3.4}$$

events where the parenthetical fraction corrects for the increased $\Delta y$ acceptance compared to that used in measuring the $\Upsilon_{1S}$ cross section. This compares favorably to the 9838 number of events that were observed before including the isolation cuts and promptness cuts of Table 1 in Ref. [25]. A cross check on the cross section is to note that the $\frac{d\sigma(\Upsilon_{1S})}{dy}\big|_{y=0} \times \mathrm{BR}(\Upsilon_{1S} \to \mu^+ \mu^-) \sim 753$ pb value measured in [30] is comparable to the estimate based on Eq. (3.4) of

$$
\begin{aligned}
&\frac{d\sigma(\Upsilon_{1S})}{dy}\bigg|_{y=0} \times \mathrm{BR}(\Upsilon_{1S} \to \mu^+ \mu^-) \\
&= \frac{\sigma(\Upsilon_{1S})_{|y|<0.6} = 34600 \text{ pb}}{\Delta y = 1.2} \times 0.0248 \sim 715 \text{ pb}.
\end{aligned} \tag{3.5}
$$

Because the earlier paper [30] may have employed slightly different procedures, efficiencies and so forth, we use the value of Eq. (3.5) at $\sqrt{s} = 1.8$ TeV.

Moving to the higher energy of $\sqrt{s} = 1.96$ TeV, it is stated in [26] that the $|y| < 0.6$ $\Upsilon_{1S}$ cross section increases relative to $\sqrt{s} = 1.8$ TeV by about 10%, implying

$$\frac{d\sigma(\Upsilon_{1S})}{dy}\bigg|_{y=0} (1.96 \text{ TeV}) \times \mathrm{BR}(\Upsilon_{1S} \to \mu^+ \mu^-) \sim 787 \text{ pb}. \tag{3.6}$$

This is the value we shall employ. As another cross check, we note that a 10% increase in the total cross section would yield about 38 330 pb at $\sqrt{s} = 1.96$ TeV. At $\sqrt{s} = 1.96$ TeV, [26] states that 52 700 $\Upsilon_{1S} \to \mu^+ \mu^-$ events are observed using the same cuts as in Ref. [25] (that imply that only an $\Upsilon_{1S}$ with $|y| < 1$ will be accepted) *and* after imposing the isolation and promptness criteria detailed in Ref. [25]. The latter imply an additional efficiency factor of 0.921 relative to the 0.066 efficiency referenced earlier. Multiplying these two efficiencies yields a net efficiency of $\sim 0.061$. With the 10% cross section increase and accounting for the increased luminosity of $L = 630 \text{ pb}^{-1}$, the 0.061 net efficiency implies an expected event number of 60 244. Although this is not in perfect agreement with the 52 700 events actually observed, we will use the result of Eq. (3.6) below.

Relative to the $\Upsilon_{1S}$ efficiency, purely geometric effects alter the efficiency for $\epsilon$ production and we assume that the same geometric changes apply to the $a$. The formula of [25] is

$$\text{efficiency}(\epsilon) = \text{efficiency}(\Upsilon_{1S})$$

$$\times \left[ 0.655 + \frac{(0.974 - 0.655)}{(9.0 - 6.3)}(m_\epsilon - 6.3) \right]. \tag{3.7}$$

We will employ this same relative efficiency for the $a$ as a function of $m_a$ using as well efficiency$(\Upsilon_{1S}) = 0.061$ as obtained above.

The most precise limits on $C_{ab\bar{b}}$ are obtained using the ratio $R$ defined in Eq. (3.3). We recall from Refs. [25,26] that the limits on $R$ are obtained by performing a smooth fit to the event distribution and looking for fluctuations about this smooth fit. The limits on the $\epsilon$ (or the $a$ in our case) are then obtained by placing small Gaussians at each possible $m_a$ value and placing limits using the observed fluctuations about the smooth fit. In the mass region for which CDF has performed this analysis, $6.3 \text{ GeV} \lesssim m_a \lesssim 9 \text{ GeV}$, it is very convenient to simply directly employ their results. As stated, we assume that the $a$ efficiencies are the same as for the $\epsilon$, in which case we can compute the ratio $R$ as

$$R \simeq \frac{\frac{d\sigma(a)}{dy}\big|_{y=0} \times \mathrm{BR}(a \to \mu^+ \mu^-)}{\frac{d\sigma(\Upsilon_{1S})}{dy}\big|_{y=0} \times \mathrm{BR}(\Upsilon_{1S} \to \mu^+ \mu^-)}, \tag{3.8}$$

where $\frac{d\sigma(a)}{dy}\big|_{y=0}$ is computed using HIGLU, $\mathrm{BR}(a \to \mu^+ \mu^-)$ is taken from Fig. 1 and $\frac{d\sigma(\Upsilon_{1S})}{dy}\big|_{y=0}\mathrm{BR}(\Upsilon_{1S} \to \mu^+ \mu^-)$ is as given in Eq. (3.6). Note that the exact values of the efficiencies, Eq. (3.7), are not important using this procedure so long as the efficiency for the $a$ is the same as for the $\epsilon$.

With these assumptions and inputs we can then predict the ratio $R$ for the case of $\epsilon = a$ and compare to the 90% CL upper limits of [26] based on $L = 630 \text{ pb}^{-1}$ of analyzed CDF data. This comparison appears in Fig. 4 for a number of $C_{ab\bar{b}} = \cos\theta_A \tan\beta$ choices. We observe that the predicted $R$ depends almost entirely on $|C_{ab\bar{b}}|$, with extremely little dependence on $\tan\beta$ separately for the $\tan\beta \gtrsim 1$, $m_a \gtrsim 4$ GeV parameter region on which we focus. The corresponding bin-by-bin limits on $|C_{ab\bar{b}}|$ obtained by interpolation appear in Fig. 5. In the 2HDM(II), they are limits on $\tan\beta = C_{ab\bar{b}}$. In the NMSSM, these are limits on $C_{ab\bar{b}} = \cos\theta_A \tan\beta$. In both cases, the interpolations are only accurate for $\tan\beta \gtrsim 1$ and $m_a \gtrsim 4$ GeV. From Fig. 5, we find that the limits based on the existing $L = 630 \text{ pb}^{-1}$ analysis roughly exclude $|C_{ab\bar{b}}| > 3$ for $6.8 \lesssim m_a \lesssim 9$ GeV and $|C_{ab\bar{b}}| > 2$ for $8.2 \lesssim m_a \lesssim 9$ GeV, but do not exclude $C_{ab\bar{b}} = 1$ for any of the $m_a$ values in the analysis range. In the 2HDM(II) case the $C_{ab\bar{b}} = \tan\beta$ limits from the Tevatron are stronger than those from Upsilon decays and LEP data, as summarized
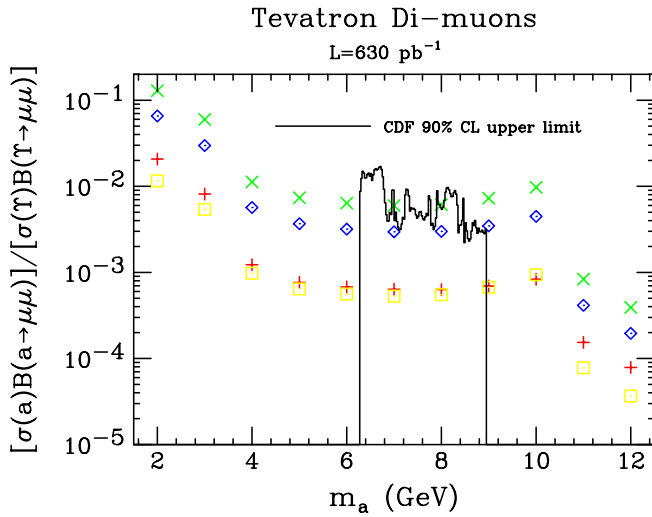
## Tevatron Di−muons

L=630 pb$^{-1}$



FIG. 4 (color online).   We plot the 90% CL limits on the ratio $R$ for $a$ production at the Tevatron as a function of $m_a$ compared to NMSSM predictions using HIGLU for the following cases: ($\tan\beta = 1$,  $\cos\theta_A = 1$) (red $+'s$), ($\tan\beta = 2$,  $\cos\theta_A = 1$) (blue  diamonds), ($\tan\beta = 3$,  $\cos\theta_A = 1$) (green $+'s$) and ($\tan\beta = 10$, $\cos\theta_A = 0.1$) (yellow squares).

earlier, for 8 GeV $\lesssim m_a \lesssim$ 9 GeV. In the NMSSM case the limits on $|\cos\theta_A|$ from the Tevatron data are the stronger in much the same mass range, as we detail shortly. In Fig. 5 we also plot the statistically extrapolated limits that would result by increasing the data sample to $L = 10$ fb$^{-1}$. (Presumably, a real analysis of a high luminosity data set would do even better.) Since the $a$ signal cross section varies roughly as $(C_{ab\bar{b}})^2$, even this large luminosity increase leads to limits that are improved by only a
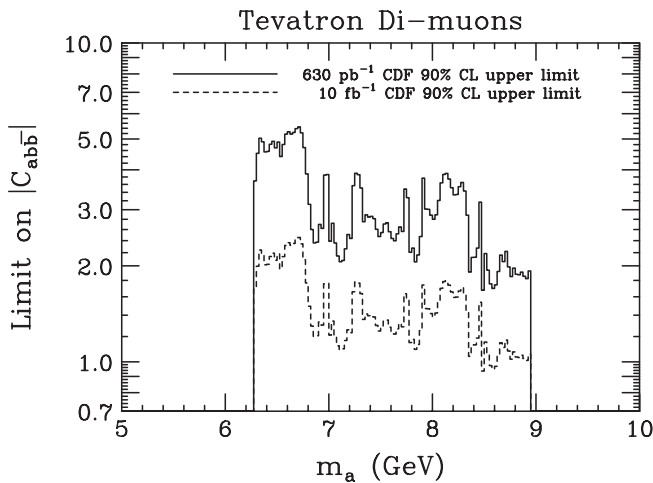
## Tevatron Di−muons



FIG. 5.   We plot the 90% CL upper limits on $|C_{ab\bar{b}}|$ obtained using the results for the ratio $R$ of Fig. 4. The 10 fb$^{-1}$ results are obtained by statistical extrapolation of the 630 fb$^{-1}$ results. In the context of the 2HDM(II), $C_{ab\bar{b}} = \tan\beta$. In the context of the NMSSM, $C_{ab\bar{b}} = \cos\theta_A \tan\beta$. In both cases, limits were derived assuming $\tan\beta \geq 1$.

factor of a bit more than two. Nonetheless, one approaches the $|C_{ab\bar{b}}| \sim 1$ level of interest in the NMSSM at $m_a = 9$ GeV.

Focusing now on the NMSSM, we compute the upper limit on $\cos\theta_A$, $\cos\theta_A^{\max}$, obtained by appropriate interpolation of the results of Fig. 4. We again emphasize that although BR($a \to \mu^+\mu^-$) is $\tan\beta$ dependent as shown in Fig. 1, it is nonetheless the case that for $\tan\beta \geq 1$ and $m_a \gtrsim 4$ GeV the limits on $C_{ab\bar{b}} = \cos\theta_A \tan\beta$ are almost independent of $\tan\beta$ at fixed $C_{ab\bar{b}}$, as found in Fig. 4 (compare the two $\cos\theta_A \tan\beta = 1$ cases — $\tan\beta = \cos\theta_A = 1$ vs $\tan\beta = 10$, $\cos\theta_A = 0.1$). This can be understood as follows. At low $\tan\beta$, although BR($a \to \mu^+\mu^-$) is suppressed, contributions to the $gga$ coupling from loops involving the top quark are substantial relative to loops involving the bottom quark. In comparison, at large $\tan\beta$ one finds that BR($a \to \mu^+\mu^-$) is maximal but top-quark loops are relatively suppressed compared to bottom quark loops. These two effects very nearly cancel one another leaving the net $a$ cross section unchanged at fixed $C_{ab\bar{b}} = \cos\theta_A \tan\beta$. As a result, it is easy to extract the $\cos\theta_A^{\max}$ values for different $\tan\beta$ values directly from the plotted limit on $|C_{ab\bar{b}}|$ shown in Fig. 5.

The resulting $\cos\theta_A^{\max}$ limits are shown in Fig. 6 in comparison to the upper limits plotted earlier in Fig. 2. The figure focuses on the 6 GeV $\lesssim m_a \lesssim$ 9 GeV region for which we have extracted the Tevatron limits using $R$. What we observe is that the 630 pb$^{-1}$ 90% CL limits become the strongest for $m_a \gtrsim 8.3$ GeV. In a forthcoming
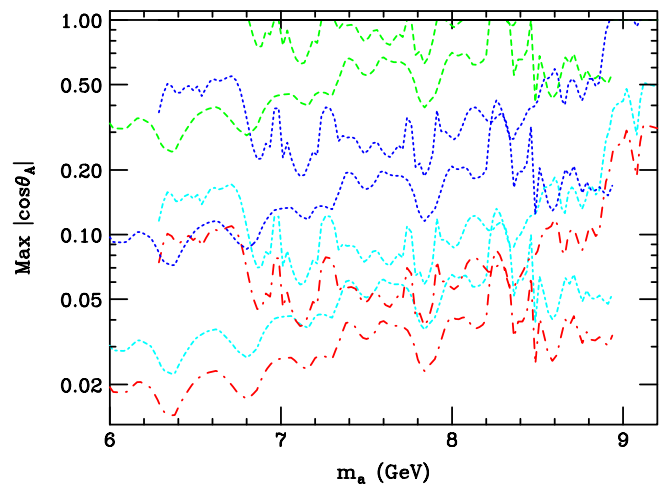


FIG. 6 (color online).   We plot the 90% CL $\cos\theta_A^{\max}$ values in the NMSSM context obtained from the results of Fig. 4 for the 630 pb$^{-1}$ CDF data set, in comparison to the $\cos\theta_A^{\max}$ values plotted in Fig. 2. For clarity, the plot is limited to the $m_a$ region over which the Tevatron data are relevant. The curve types are as in Fig. 2. The Fig. 2 results for a given curve type are those for which $\cos\theta_A^{\max}$ starts at lower values at low $m_a$ rising to higher values at higher $m_a$. The new CDF limits are those that begin near $m_a \sim 6.3$ GeV and terminate at $m_a \sim 9$ GeV and that fall (with fluctuations) as $m_a$ increases.

paper, we will analyze the impact of *BABAR* data for $\Upsilon_{3S} \to \gamma\tau^+\tau^-$ decays on the 6 GeV $\lesssim m_a \lesssim$ 10 GeV region. Our preliminary results suggest that the Tevatron limits plotted above and the $\Upsilon_{3S}$ limits are very similar at $m_a \sim 9$ GeV, with $\Upsilon_{3S}$ limits being superior for lower $m_a$.

Given the above, the great value of extending the Tevatron analysis above $M_{\mu^+\mu^-} = 9$ GeV is apparent. A full analysis of existing and future data all the way out to $m_a \sim 12$ GeV is needed. First, it might strongly constrain the properties of any light $a$ with $m_a \lesssim 2m_B$ that would allow for the ideal Higgs scenario. Second, it might completely eliminate the possibility that a light $a$ could provide a major contribution to $a_\mu$. At the moment, the Tevatron limits on $C_{ab\bar{b}}$ shown rule out a significant contribution to $\Delta a_\mu$ from an $a$ with $m_a < 9$ GeV, while in the range 9 GeV $\lesssim m_a \lesssim 2m_B$ these limits leave open the possibility of $\Delta a_\mu$ arising from diagrams involving a $CP$-odd $a$. Only the Tevatron and/or LHC can probe the region of $m_a$ above the Upsilon masses.

Absent a full analysis by CDF of limits on $R$ in the region $M_{\mu^+\mu^-} > 9$ GeV and given that this region is of great interest, we wish to make some estimates of limits on $|C_{ab\bar{b}}|$ based on the event number plots of Ref. [26]. We have employed the following procedure. First, for this analysis, we must know the efficiency for detecting the $a$. For our estimates we use efficiency($m_a$) from Eq. (3.7) and efficiency($\Upsilon_{1S}$) = 0.061 [as motivated earlier below Eq. (3.6)] to predict the number of $a$ events as a function of $m_a$. Second, we wish to determine how many of the total number of $a$ events fall into a 50 MeV bin centered on $m_a$. To do so, we need to know the resolution as a function of $m_a$. In [26], it is stated that the resolution, $\sigma_r$ varies from 32 MeV to 50 MeV in going from $m_a = 6.3$ GeV to $m_a = 9$ GeV, with a value of 52 MeV at $M_{\Upsilon_{1S}}$. We use a simple linear interpolation for other values of $m_a$, but do not allow $\sigma_r$ to fall below 25 MeV at low $m_a$. The fraction of $a$ events distributed as a Gaussian of width $\sigma_r$ that fall into a 50 MeV bin (which should be thought of as a bin of half width 25 MeV) that is centered on $m_a$ is given by

$$f(m) = \text{Erf}\left(\frac{25 \text{ MeV}}{\sqrt{2}\sigma_r(m)}\right), \tag{3.9}$$

where $\sigma_r(m)$ is in MeV. In Fig. 7, we plot the 1.646$\sigma$, i.e. 90% CL, fluctuation number for each of the CDF 50 MeV bins compared to the predicted number of $a$ events that would fall into that bin. We do this for the same selection of $(\tan\beta, \cos\theta_A)$ values as employed in Fig. 4. One observes that for $m_a \sim 6$ GeV ($m_a \sim 9$ GeV) 90% CL sensitivity is anticipated for $C_{ab\bar{b}} \gtrsim 3$ ($C_{ab\bar{b}} \gtrsim 2$). This anticipates in an average sense the more precise (and more fluctuating) results based on the $R$ analysis found in Fig. 5.

Sensitivity to the $a$ in the $S/\sqrt{B}$ sense can actually be improved by taking a bin size that properly matches $\sigma_r$. If the background is flat then the optimal bin size is $2\sqrt{2}\sigma_r$ which retains a fraction Erf(1) = 0.843 of the total $a$ signal
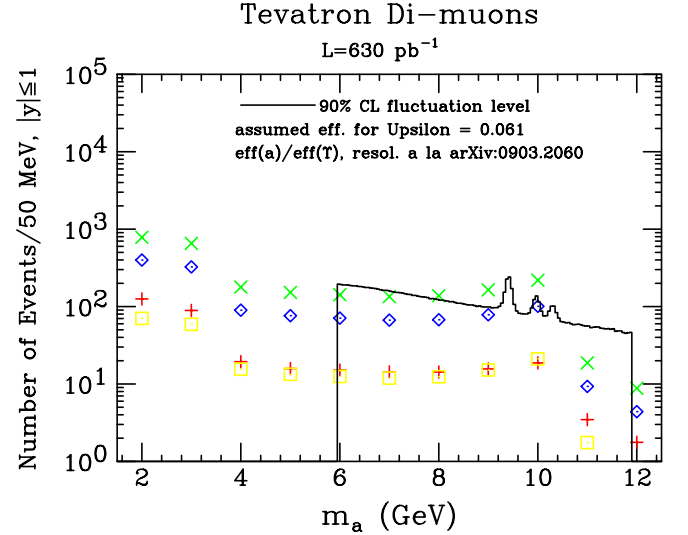


FIG. 7 (color online). We plot the upwards fluctuation in the number of events in a given bin corresponding to a 1.646$\sigma$ (90% CL) excess as predicted using the $L = 630$ pb$^{-1}$ event numbers of [26]. These limits are compared to the predicted number of events for an $a$ resonance centered on that bin spread out by the experimental resolution. The same $(\tan\beta, \cos\theta_A)$ values as in Fig. 4 are considered.

and yields $B = 2\sqrt{2}\sigma_r \frac{d\sigma_B}{dM_{\mu^+\mu^-}}$. Following this procedure we can then use interpolation to extract the $|C_{ab\bar{b}}|$ value such that $S/\sqrt{B}$ is 1.646. The resulting values of $|C_{ab\bar{b}}|$ which correspond to this 90 CL fluctuation in the $\Delta M_{\mu^+\mu^-} = 2\sqrt{2}\sigma_r$ acceptance window are plotted in Fig. 8. As anticipated above, this event counting method turns out to give a good average representation of the results obtained using $R$ (which analysis was based on bin-by-bin fits of the fluctuations about a smooth curve) at the 90% CL. Thus, despite relatively small $S/B$ levels (typically of order 0.02 in each of two neighboring bins for a 1.646$\sigma$ net fluctuation), our estimates for expectations for $m_a > 9$ GeV (using the approach of assuming there were no 1.646$\sigma$ fluctuations in the absolute $L = 630$ pb$^{-1}$ event numbers in acceptance windows of size $\Delta M_{\mu^+\mu^-}$) should give a good idea of the limits that are implicit in current data.

As an aside, we note that even though the shape of the $\Upsilon(nS)$ resonances (which are also very narrow) will also be determined by $\sigma_r$, one can learn if there is an excess in the $\mu^+\mu^-$ final state by also looking at the $\Upsilon(nS)$ resonance in the $e^+e^-$ final state to which the $a$ will not contribute. Assuming lepton universality, the $\Upsilon(nS)$ contribution in the $\mu^+\mu^-$ final state can be subtracted from the $\mu^+\mu^-$ spectrum, after which any residual excess from the presence of an $a$ would become apparent. Statistical errors resulting from this subtraction will be roughly a factor of $\sqrt{2}$ larger than employed above. However, this procedure does rely on a precise understanding of efficiencies, reso-
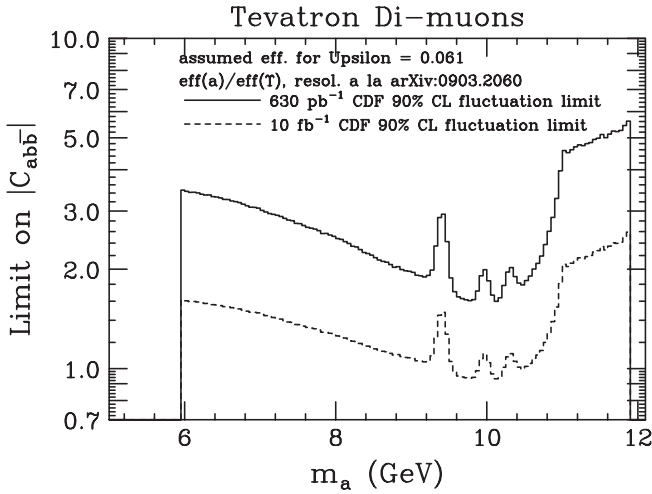
FIG. 8. We plot approximate limits on $|C_{ab\bar{b}}|$ as a function of $m_a$ estimated assuming that bins centered on $m_a$ and encompassing an $m_a$ range of $2\sqrt{2} \times \sigma_r$, where $\sigma_r$ is the experimental $M_{\mu^+\mu^-}$ resolution at the given $m_a$, do not have a 90% CL fluctuation relative to the number of events observed and plotted over this bin range in [26] for $L = 630$ pb$^{-1}$. The $L = 10$ fb$^{-1}$ histogram corresponds to simply scaling the predicted $a$ event rate and the 90% CL fluctuations to the increased luminosity.



FIG. 9 (color online). We plot the upwards fluctuation in the number of events in a given bin corresponding to a $1.646\sigma$ (90% CL) excess as predicted using the $L = 630$ pb$^{-1}$ event numbers of [26] scaled up to $L = 10$ fb$^{-1}$. These limits are compared to the predicted number of events for $L = 10$ fb$^{-1}$ for an $a$ resonance centered on that bin spread out by the experimental resolution. The same $(\tan\beta, \cos\theta_A)$ values as in Fig. 4 are considered.

lutions and the like for electrons. Another technique that could be considered is comparing one Upsilon resonance to another. If the relative normalization between the two Upsilon resonances can be sufficiently precisely predicted, including both theoretical and experimental uncertainties, then an $a \rightarrow \mu^+\mu^-$ signal hiding under one of the Upsilons could become apparent.

Both CDF and D0 will continue to accumulate data far in excess of $L = 630$ pb$^{-1}$. Thus, it is useful to extrapolate to higher luminosity using the observed number of events for $L = 630$ pb$^{-1}$ plotted in [26]. We rescale the observed number of events in each bin to $L = 10$ fb$^{-1}$ and compute the 90% CL fluctuation upper limit in each bin as $1.646 \times \sqrt{N_{\text{evt}}(\text{bin})}$. In Fig. 9, we plot these extrapolated $1.646\sigma$ fluctuation levels in each bin compared to the predicted number of $a$ events in each bin for the same selection of $(\tan\beta, \cos\theta_A)$ values as employed in Fig. 4. The extracted limits on $|C_{ab\bar{b}}|$ are plotted in Fig. 8. We see that the eventual Tevatron limits from just one experiment could easily be superior to those currently available from Upsilon decays, in particular, probing the $C_{ab\bar{b}} = \cos\theta_A \tan\beta \lesssim 1$ coupling level, of particular interest for the ideal Higgs scenario, all the way up to $m_a = 2m_B$, except in the vicinity of the Upsilon peaks.

Some further comments are the following. First, we emphasize that the $1.646\sigma$ approximate procedure leads to the expectation that quite important limits are possible for $L = 10$ fb$^{-1}$ in the $9$ GeV $\lesssim m_a \lesssim 2m_B$ region of great interest in the NMSSM version of the ideal Higgs scenario for which $m_a \gtrsim 8$ and $|C_{ab\bar{b}}| \sim 0.2$–$2$ is a
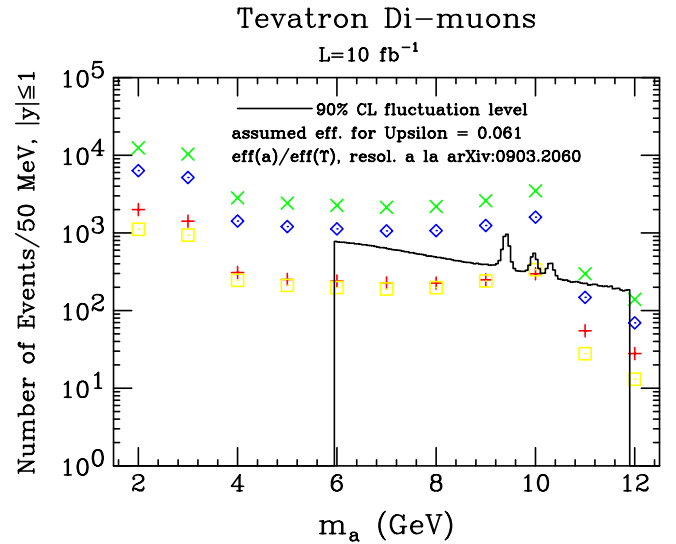
strongly preferred parameter region. If this scenario were to be nature's choice, there is a decent chance of observing an $a$ using the dimuon spectrum analysis and the ultimate Tevatron data set.

Second, we again note that even the $L = 630$ pb$^{-1}$ estimated limits of Fig. 8 for $9$ GeV $\leq m_a \leq 12$ GeV would rule out the enhanced $|C_{ab\bar{b}}|$ values of order $30$ needed for $a$-exchange graphs to explain the $a_\mu$ discrepancy for $m_a$ in this mass region, which is the only relatively low mass region for which other current constraints are sufficiently weak that the $a$ might provide the observed discrepancy. It is thus quite important for CDF (and D0) to perform the needed analysis using the $R$ or similar technique and determine whether or not the rough limits we obtained above using event numbers are approximately correct.

## IV. LHC PROSPECTS

The basic question is whether the LHC will be able to improve over the Tevatron $L = 10$ fb$^{-1}$ projected results and limits. The total cross sections at the LHC appear in Figs. 10 and 11 for $\sqrt{s} = 14$ TeV and $\sqrt{s} = 10$ TeV respectively; they are plotted analogously to those for the Tevatron appearing in Fig. 3. Recall that these cross sections are those appropriate in the 2HDM(II) context. We see that, relative to the Tevatron, the $\sqrt{s} = 14$ TeV cross sections are about a factor of 3–7 higher, the smaller (larger) ratio applying at small (large) $m_a$. Relative to the
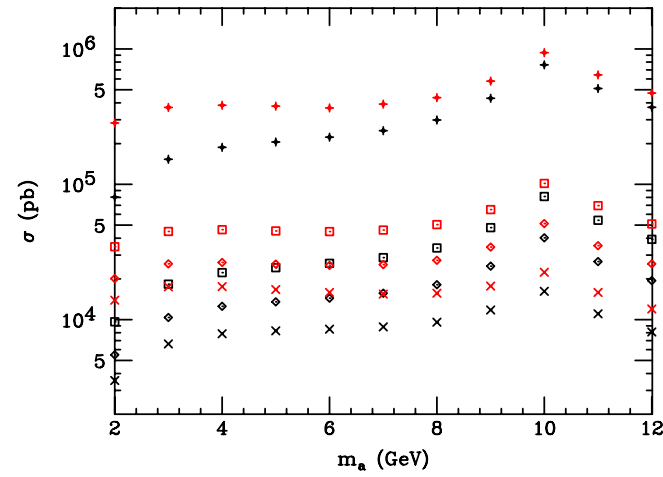
FIG. 10 (color online). The total cross section for $a$ production at the LHC for $\sqrt{s} = 14$ TeV is plotted vs $m_a$ for $\tan\beta = 1, 2, 3, 10$ (lowest to highest point sets). For each $m_a$ and $\tan\beta$ value, the lower (higher) point is the cross section without (with) resolvable parton final state contributions.
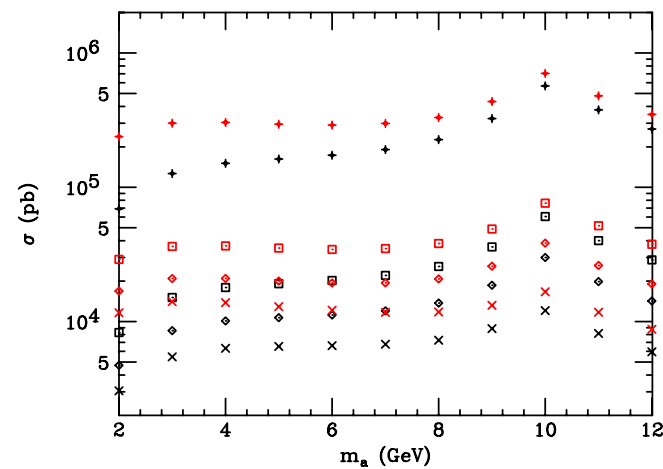


FIG. 12 (color online). The total cross section for $a$ production at the LHC for $\sqrt{s} = 7$ TeV is plotted vs $m_a$ for $\tan\beta = 1, 2, 3, 10$ (lowest to highest point sets). For each $m_a$ and $\tan\beta$ value, the lower (higher) point is the cross section without (with) resolvable parton final state contributions.
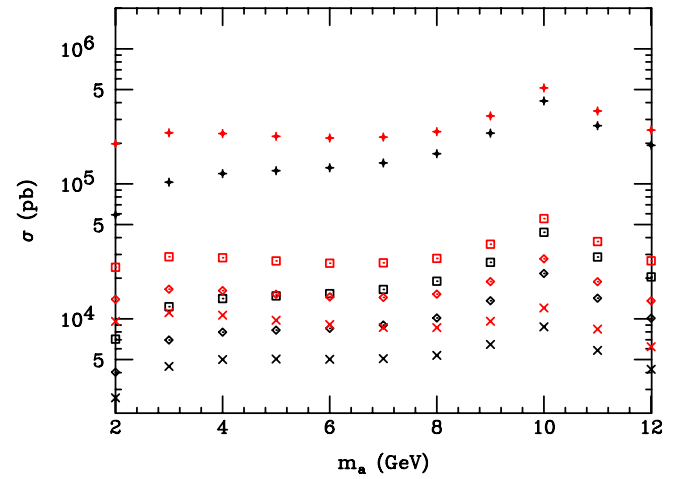
$\sqrt{s} = 14$ TeV cross section, the $\sqrt{s} = 10$ TeV cross sections are roughly a factor of $\sim 1.2$ smaller at $m_a = 2$ GeV and a factor $\sim 1.34$ smaller at $m_a = 10$ GeV, more or less independent of the $\tan\beta$ value. It now appears that perhaps as much as a year will be spent running at $\sqrt{s} = 7$ TeV. Thus, we also plot in Fig. 12 the cross sections for this latter energy. At $m_a = 2$ GeV, the $a$ cross section at $\sqrt{s} = 10$ TeV is a factor of about 1.15 larger than the $\sqrt{s} = 7$ TeV cross section; the factor rises to $\sim 1.35$ for $m_a = 10$ GeV. The modest decrease of the $a$ cross section with decreasing energy is a result of the fact that the $gg$ luminosity at low $m_a$ varies slowly with $\sqrt{s}$. This is one of the

reasons why searches for a light $a$ are very appropriate in early LHC running.

In going to the NMSSM, one takes these results for any given $\tan\beta$ choice and then multiplies by $(\cos\theta_A)^2$, the square of the overlap fraction of the $a$ with the 2HDM component.

As an example of how limits obtained at the LHC in early running will compare to the Tevatron limits, let us consider the case of $\tan\beta = 10$ and $\cos\theta_A = 0.1$, for which $C_{ab\bar{b}} = 1$. As shown in Fig. 8, even with $L = 10$ fb$^{-1}$ the Tevatron is not fully able to probe at the 90% CL the predicted relatively small $a$ event levels except at $m_a$ values close to $2m_B$ but outside the $\Upsilon(nS)$ peaks. In more detail, for the above parameter choices, the predicted number of $a \to \mu^+\mu^-$ events for $|y| \leq 1$ in a $\Delta M_{\mu^+\mu^-} = 2\sqrt{2}\sigma_r$ bin centered on $m_a$ is 436, 615 and 475 at $m_a = 8$ GeV, $M_{\Upsilon_{1S}}$ and 10.5 GeV, respectively, where the event numbers quoted incorporate the Erf$(1) = 0.8427$ reduction factor associated with keeping only events in an interval of size $\Delta M_{\mu^+\mu^-} = 2\sqrt{2}\sigma_r$. The actual $\Delta M_{\mu^+\mu^-} = 2\sqrt{2}\sigma_r$ values are 43 MeV, 52 MeV, and 57 MeV at 8 GeV, $M_{\Upsilon_{1S}}$, and 10.5 GeV, respectively. As regards the background, we take the 50 MeV bin event numbers in the CDF plot of the number of events in each bin and rescale to the $\Delta M_{\mu^+\mu^-}$ interval sizes at the above $M_{\mu^+\mu^-} = m_a$ choices. This gives us a background event number $N_{\Delta M_{\mu^+\mu^-}}$ at each $m_a$. The $1\sigma$ fluctuations in these background event numbers, $\sqrt{N_{\Delta M_{\mu^+\mu^-}}}$, are 468, 945, and 285, respectively. The statistical significances of the $a$ signals are then $\sim 0.93\sigma$, $\sim 0.65\sigma$, and $\sim 1.67\sigma$, respectively. Only the latter is (slightly) above the $1.646\sigma$ level corresponding to 90% CL. However, to repeat, this high $m_a \lesssim 2m_B$ region



FIG. 11 (color online). The total cross section for $a$ production at the LHC for $\sqrt{s} = 10$ TeV is plotted vs $m_a$ for $\tan\beta = 1, 2, 3, 10$ (lowest to highest point sets). For each $m_a$ and $\tan\beta$ value, the lower (higher) point is the cross section without (with) resolvable parton final state contributions.

is particularly favored in the model context. But, to reach $5\sigma$ at $m_a = 10.5$ GeV would require about 9 times as much integrated luminosity, i.e. $L \sim 90$ fb$^{-1}$ and $5\sigma$ at $m_a = M_{\Upsilon_{1S}}$ would require $L \sim 590$ fb$^{-1}$.

Projections for the LHC have been made public by ATLAS. In Fig. 1 of [31], one finds a plot of $d\sigma/dM_{\mu^+\mu^-}$ coming from $b\bar{b}$ production, Drell-Yan production and $\Upsilon_{1S}$ production. The dimuon Drell-Yan contribution is negligible compared to that from $b\bar{b}$ production even after the latter is reduced by muon isolation requirements. We ignore the Drell-Yan contribution in all subsequent discussions.

In generating the $b\bar{b}$ and $\Upsilon_{1S}$ cross sections, only events with $p_T$ cuts requiring one muon with $p_T > 6$ GeV and a 2nd muon with $p_T > 4$ GeV, both with $|\eta| < 2.4$, were retained. A recent Monte Carlo study [32] finds that these events constitute 20% of the total inclusive cross section. The fraction of these events that survive after further requirements related to triggering, reconstruction and the final analysis selection cuts is 50%. Thus, the net efficiency for the $\Upsilon_{1S}$ events plotted in Fig. 1 of [31] is $\sim 0.5 \times 0.2 = 0.1$. Therefore, we will write $\epsilon_{\text{ATLAS}} = 0.1r$ for the fraction of inclusive $a$ events that will be retained, where $r \sim 1$ for the cuts and triggering strategies studied so far, but $r > 1$ is probably achievable if these are optimized for the *CP*-odd $a$.

Returning to Fig. 1 of [31], we observe a $b\bar{b}$-induced dimuon cross section level for $\sqrt{s} = 14$ TeV of order $d\sigma/dM_{\mu^+\mu^-} \sim 50\text{–}90$ pb/100 MeV in the $M_{\mu^+\mu^-} \in$ [8 GeV, $2m_B$] interval when outside the Upsilon peak region. This is the dimuon cross section from $b\bar{b}$ heavy flavor production only. The author of [31] estimates [33] that one should at most double this cross section to account for $c\bar{c}$ production and other contributions. We will make estimates based on multiplying the $b\bar{b}$-induced dimuon cross section by a factor of 2. To this, we add the $\Upsilon_{1S}$ cross section as plotted in Fig. 1. The net resulting spectrum constitutes the background to the $a$ signal that we discuss shortly.

As in the CDF case, we will use a bin size of $\Delta_{M_{\mu^+\mu^-}} = 2\sqrt{2}\sigma_r$ (which optimizes $S/\sqrt{B}$ for a flat background) for comparing the $a$ signal to the above stipulated background. As for resolutions, it is stated in [31] that the resolution at the $J/\psi$ is around 54 MeV while that at the $\Upsilon_{1S}$ is close to 170 MeV. We use a linear interpolation for other values of $M_{\mu^+\mu^-}$. Assuming $L = 10$ pb$^{-1}$ of integrated luminosity, the background event numbers $N_{\Delta_{M_{\mu^+\mu^-}}}$ in the intervals of size $\Delta_{M_{\mu^+\mu^-}} = 2\sqrt{2}\sigma_r$ are 4055 at $m_a = 8$ GeV, 50 968 at $m_a = M_{\Upsilon_{1S}}$, and 9620 at $m_a = 10.5$ GeV. We take the square root to determine the $1\sigma$ fluctuation level.

We now consider the $a \to \mu^+\mu^-$ signal rates. From Fig. 10, we see that at $\tan\beta = 10$ the total $a$ cross section ranges from about $4.2 \times 10^5$ pb$(\cos\theta_A)^2 \sim 4200$ pb at $m_a = 8$ GeV to $\sim 8500$ pb at $m_a \lesssim 2m_B$ for

$\sqrt{s} = 14$ TeV. The cross section for $a \to \mu^+\mu^-$ assuming $\tan\beta = 10$ and $\cos\theta_A = 0.1$ will then range from $4200\text{–}8500$ pb $\times$ (BR$(a \to \mu^+\mu^-) \sim 0.003) \sim 12\text{–}25$ pb. As discussed above, we will write the total $a$ efficiency in the form $\epsilon_{\text{ATLAS}} = 0.1 \times r$. Multiplying the above cross section by $\epsilon_{\text{ATLAS}}$ and by the Erf(1) = 0.8427 acceptance factor for the ideal interval being employed and using $L = 10$ pb$^{-1}$ (as employed above in computing the number of background events), we obtain $a$ event numbers of $10 \times r$, $18.5 \times r$ and $21 \times r$ at $m_a = 8$ GeV, $M_{\Upsilon_{1S}}$, and 10.5 GeV, respectively. The statistical significances of the $a$ peaks for $L = 10$ pb$^{-1}$ are then $r\times$ the $r = 1$ results of $0.16\sigma$, $0.08\sigma$, and $0.22\sigma$, respectively.

Of course, we currently expect that substantial early running will mostly take place at $\sqrt{s} = 7$ TeV and $\sqrt{s} = 10$ TeV. As noted earlier, lower $\sqrt{s}$ implies a somewhat smaller $a$ cross section in the [8 GeV, $2m_B$] mass interval on which we are focusing. Roughly, relative to $\sqrt{s} = 14$ TeV, the $a$ cross section decreases by a factor of $\sim 1.3$ at $\sqrt{s} = 10$ TeV and a factor of $\sim 1.7$ at $\sqrt{s} = 7$ TeV in this mass interval. Since the backgrounds are also basically $gg$ fusion induced, we presume that these same factors will apply to them. At $\sqrt{s} = 10$ TeV ($\sqrt{s} = 7$ TeV) this then will reduce the statistical significances given above by a factor of $1/\sqrt{1.3}$ ($1/\sqrt{1.7}$). The statistical significances at $m_a = 8$ GeV, $M_{\Upsilon_{1S}}$ and 10.5 GeV are, respectively, then $0.14\sigma$, $0.07\sigma$, $0.19\sigma$ at 10 TeV and $0.12\sigma$, $0.06\sigma$, $0.17\sigma$ at 7 TeV, all to be multiplied by $r$.

Given the above results, we can tabulate the integrated luminosity $L$ needed to achieve a $5\sigma$ significance at each of the three energies. The results appear in Table II. The required $L$'s away from the Upsilon resonance may be achieved after a year or two of LHC operation. The sensitivity of the required luminosities to $r$ shows the importance of firmly establishing the precise efficiencies for background and signal. We look forward to continued and detailed work by the ATLAS collaboration in this area. Of course, we must not forget that the required $L$'s are very sensitive to $\tan\beta$, $\cos\theta_A$ and BR$(a \to \mu^+\mu^-)$; very roughly for $\tan\beta \neq 10$, $\cos\theta_A \neq 0.1$ and/or BR$(a \to \mu^+\mu^-) \neq 0.003$ the tabulated luminosities need to be multiplied by

$$\left(\frac{0.003}{\text{BR}(a \to \mu^+\mu^-)}\right)^2 \left(\frac{1}{\cos\theta_A}\right)^4 \left(\frac{10}{(\tan\beta)^{1.6-1.8}}\right)^2, \quad (4.1)$$

where the 1.6 applies for $m_a \sim 8$ GeV and the 1.8 applies

TABLE II. Luminosities (fb$^{-1}$) needed for $5\sigma$ if $\tan\beta = 10$ and $\cos\theta_A = 0.1$.

| Case | $m_a = 8$ GeV | $m_a = M_{\Upsilon_{1S}}$ | $m_a \lesssim 2m_B$ |
|---|---|---|---|
| ATLAS LHC7 | $17/r^2$ | $63/r^2$ | $9/r^2$ |
| ATLAS LHC10 | $13/r^2$ | $48/r^2$ | $7/r^2$ |
| ATLAS LHC14 | $10/r^2$ | $37/r^2$ | $5.4/r^2$ |

for $m_a \lesssim 2m_B$. Depending upon the precise value of $m_a$ and $\tan\beta$, in the $m_a$ mass range under discussion Fig. 1 shows that BR($a \to \mu^+\mu^-$) can range from a low of 0.0023 at $\tan\beta = 1.5$ and $m_a \lesssim 2m_B$ to a high of 0.0033 for $\tan\beta \gtrsim 3$ and $m_a = 8$ GeV. The minimum values of $\cos\theta_A$, with and without placing a maximum on the light-$a$ finetuning measure $G$, were detailed in Table I.

Studies by CMS analogous to the ATLAS studies discussed above are under way [34].

## V. CONCLUSIONS

In this paper we have shown that a dedicated analysis of the dimuon spectrum at the Tevatron and LHC at low masses, i.e. $M_{\mu^+\mu^-} \lesssim 2m_B$, will provide very important constraints on models containing a light $CP$-odd Higgs boson. We employed the published $L = 630$ pb$^{-1}$ CDF analysis of the dimuon spectrum between $\sim 6.3$ GeV and 9 GeV by CDF and found that constraints on the $b\bar{b}a$ coupling $C_{ab\bar{b}}$ become competitive with those from $\Upsilon(nS) \to \gamma a$ decays for 8.5 GeV $\lesssim m_a \lesssim 9$ GeV, and will be superior for larger data sets. In addition, only hadron colliders have the kinematic reach to constrain $|C_{ab\bar{b}}|$ in the important region $M_{\Upsilon_{3s}} \lesssim m_a \lesssim 2m_B$. In particular, for $L = 10$ fb$^{-1}$, the Tevatron will provide significant constraints on the $|C_{ab\bar{b}}| \gtrsim 1$ portion of the 8 GeV $\lesssim m_a \lesssim 2m_B$ mass region that would allow an NMSSM ideal Higgs scenario with an $m_h \sim$ 100–105 GeV $CP$-even $h$ decaying primarily via $h \to aa \to \tau^+\tau^-\tau^+\tau^-$ to be possible with neither electroweak fine-tuning nor "light-$a$" fine-tuning. It is also very noteworthy that our rough estimates of the limits that CDF could place on $|C_{ab\bar{b}}|$ using the $L = 630$ fb$^{-1}$ event rates in the $9 \leq m_a \leq 12$ GeV region are such that the observed $a_\mu$ discrepancy could not be explained by a light $a$.

For the LHC, we have obtained rough estimates of what will be possible using information available from the ATLAS collaboration, in particular, regarding the efficiency (for triggering, tracking, $p_T$ cuts, etc.) for retaining $a \to \mu^+\mu^-$ events. We find that it will be possible to obtain a $5\sigma$ signal for a light $a$ with $\tan\beta \sim 10$ and $\cos\theta_A \sim 0.1$ throughout the entire range 8 GeV $\lesssim m_a \lesssim 2m_B$ away from the Upsilon peaks for $L \sim 13$ fb$^{-1}$ at $\sqrt{s} = 10$ TeV or $L \sim 17$ fb$^{-1}$ at $\sqrt{s} = 7$ TeV. For ex-

ample, at $m_a = 10.5$ GeV, only $L \sim 7$ fb$^{-1}$ at $\sqrt{s} = 10$ TeV or $L \sim 9$ fb$^{-1}$ at $\sqrt{s} = 7$ TeV is required to achieve a $5\sigma$ signal for such an $a$.

Of course, not all acceptable NMSSM models have $|C_{ab\bar{b}}|$ as large as $\sim 1$. As an extreme example, at $\tan\beta = 1.7$, $\cos\theta_A \sim 0.1$ is possible for small light-$a$ fine-tuning (corresponding to $C_{ab\bar{b}} \sim 0.17$). In this case, the $a$ cross section at $m_a \lesssim 2m_B$ is about a factor of 18 smaller than at $\tan\beta = 10$ and $\cos\theta_A \sim 0.1$. Using statistical extrapolation this suggests that as much as 324 times more luminosity would be needed to achieve the same statistical significances as above. However, one should keep in mind that it may in the end be possible to obtain net efficiencies for the $a$ at ATLAS and CMS in excess of the current ATLAS estimate of 10%. Indeed, early CMS studies suggest that net efficiencies might be as high as 30% [34]. Since the needed $L$ scales inversely with the square of the efficiency, assuming $\sqrt{s} = 14$ TeV and $r = 3$ one finds that a $5\sigma$ signal could be achieved for $\tan\beta = 1.7$ and $\cos\theta_A \sim 0.1$ with $L \sim 195$ fb$^{-1}$, an integrated luminosity that should be achieved in the not too distant future, although background levels might be larger at the higher instantaneous luminosities needed to achieve such large total $L$.

Overall, this kind of search is quite important given that there are many models in which light $a$'s are present that have significant, even if not enhanced, couplings to gluons via quark loops and that would have reasonable $a \to \mu^+\mu^-$ branching ratio. Searching for such $a$'s and constraining their possible masses and couplings is an important general goal and both Tevatron and LHC data will be of great value.

[1] R. Dermisek and J. F. Gunion, Phys. Rev. Lett. **95,** 041801 (2005).

[2] R. Dermisek and J. F. Gunion, Phys. Rev. D **73,** 111701 (2006).

[3] R. Dermisek and J. F. Gunion, Phys. Rev. D **75,** 075019 (2007).

[4] R. Dermisek and J. F. Gunion, Phys. Rev. D **76,** 095006 (2007).

[5] S. Chang, P. J. Fox, and N. Weiner, J. High Energy Phys. 08 (2006) 068.

[6] S. Chang, R. Dermisek, J. F. Gunion, and N. Weiner, Annu. Rev. Nucl. Part. Sci. **58,** 75 (2008).

[7] J. F. Gunion, J. High Energy Phys. 08 (2009) 032.

[8] J. R. Ellis, J. F. Gunion, H. E. Haber, L. Roszkowski, and F. Zwirner, Phys. Rev. D **39**, 844 (1989).

[9] John F. Gunion, Howard E. Haber, Gordon Kane, and Sally Dawson, in *The Higgs Hunter's Guide*, Frontiers in Physics Vol. 80 (1990).

[10] U. Ellwanger, J. F. Gunion, and C. Hugonie, J. High Energy Phys. 02 (2005) 066.

[11] U. Ellwanger and C. Hugonie, Comput. Phys. Commun. **175**, 290 (2006).

[12] L. J. Hall, R. Rattazzi, and U. Sarid, Phys. Rev. D **50**, 7048 (1994).

[13] M. S. Carena, M. Olechowski, S. Pokorski, and C. E. M. Wagner, Nucl. Phys. **B426**, 269 (1994).

[14] D. M. Pierce, J. A. Bagger, K. T. Matchev, and R. j. Zhang, Nucl. Phys. **B491**, 3 (1997).

[15] R. Dermisek, arXiv:0806.0847.

[16] R. Dermisek, in *The 16th International Conference on Supersymmetry and the Unification of Fundamental Interactions*, edited by P. Ho and D K. Hong, AIP Conf. Proc. No. 1078 (AIP, New York, 2009), p. 226.

[17] R. Dermisek and J. F. Gunion, Phys. Rev. D **79**, 055014 (2009).

[18] R. Dermisek, Mod. Phys. Lett. A **24**, 1631 (2009).

[19] F. Domingo, U. Ellwanger, E. Fullana, C. Hugonie, and M. A. Sanchis-Lozano, J. High Energy Phys. 01 (2009) 061.

[20] R. Dermisek, J. F. Gunion, and B. McElrath, Phys. Rev. D **76**, 051105 (2007).

[21] B. Aubert *et al.* (*BABAR* Collaboration), Phys. Rev. Lett. **103**, 181801 (2009).

[22] B. Aubert *et al.* (*BABAR* Collaboration), Phys. Rev. Lett. **103**, 081803 (2009).

[23] K. Cranmer, CERN, 2009 (unpublished).

[24] R. Dermisek and J. F. Gunion, arXiv:1002.1971.

[25] G. Apollinari *et al.*, Phys. Rev. D **72**, 092003 (2005).

[26] T. Aaltonen *et al.* (CDF Collaboration), Eur. Phys. J. C **62**, 319 (2009).

[27] P. Artoisenet, J. M. Campbell, J. P. Lansberg, F. Maltoni, and F. Tramontano, Phys. Rev. Lett. **101**, 152001 (2008).

[28] E. L. Berger, J. w. Qiu, and Y. l. Wang, Phys. Rev. D **71**, 034007 (2005).

[29] M. Spira, Nucl. Instrum. Methods Phys. Res., Sect. A **389**, 357 (1997); arXiv:hep-ph/9510347.

[30] F. Abe *et al.* (CDF Collaboration), Phys. Rev. Lett. **75**, 4358 (1995).

[31] D. D. Price, arXiv:0808.3367.

[32] Based on result obtained by Yi Yang, under the direction of H. Evans.

[33] D. Price (private communication).

[34] D. Bortoletto and Z. Gecse (private communication).

[35] W. Love *et al.* (CLEO Collaboration), Phys. Rev. Lett. **101**, 151802 (2008).